

SU(N) spin-wave theory: Application to spin-orbital Mott insulators

Zhao-Yang Dong, Wei Wang, and Jian-Xin Li*

National Laboratory of Solid State Microstructures and Department of Physics, Nanjing University, Nanjing 210093, China and Collaborative Innovation Center of Advanced Microstructures, Nanjing University, Nanjing 210093, China

(Received 23 November 2017; revised manuscript received 29 April 2018; published 8 May 2018)

We present the application of the SU(N) spin-wave theory to spin-orbital Mott insulators whose ground states exhibit magnetic orders. When taking both spin and orbital degrees of freedom into account rather than projecting Hilbert space onto the Kramers doublet, which is the lowest spin-orbital locked energy levels, the SU(N) spin-wave theory should take the place of the SU(2) one due to the inevitable spin-orbital multipole exchange interactions. To implement the application, we introduce an efficient general local mean-field method, which involves all local fluctuations, and develop the SU(N) linear spin-wave theory. Our approach is tested firstly by calculating the multipolar spin-wave spectra of the SU(4) antiferromagnetic model. Then, we apply it to spin-orbital Mott insulators. It is revealed that the Hund's coupling would influence the effectiveness of the isospin-1/2 picture when the spin-orbital coupling is not large enough. We further carry out the SU(N) spin-wave calculations of two materials, α -RuCl₃ and Sr₂IrO₄, and find that the magnonic and spin-orbital excitations are consistent with experiments.

DOI: [10.1103/PhysRevB.97.205106](https://doi.org/10.1103/PhysRevB.97.205106)**I. INTRODUCTION**

The physics of transition-metal oxides (TMOs) with $4d$ or $5d$ orbitals occupied has drawn considerable attention recently. One reason is that the spin-orbital coupling (SOC), which was considered as a small perturbation until recently, entangles the spin and orbital degrees of freedom. This effect in cooperation with electronic correlations could give rise to a novel type of insulators (spin-orbital Mott insulators) in which the local moments are spin-orbital entangled $J_{\text{eff}} = 1/2$ Kramers doublet [1–3]. The underlying picture for this process is as following. For a d^5 electronic configuration, the crystal field of the octahedron splits off the two e_g orbitals, and leaves the five electrons with a total $s = 1/2$ magnetic moment on the t_{2g} orbitals with an effective $l = 1$ orbital moment. A strong SOC leads to a system with a fully filled $J_{\text{eff}} = 3/2$ band and a half-filled $J_{\text{eff}} = 1/2$ band. Thus, the so-called spin-orbital Mott insulators emerge even with a relatively small electronic correlation. The other is their crystal structures with a special bond geometry formed by edge-shared octahedra, which will result in the anisotropy and frustration of the effective Hamiltonian [4], because the exchange coupling between local moments depends highly on the spatial direction of the exchange path. The Hamiltonian with such spin exchange couplings could lead to unconventional magnetism, including multipolar orders, spin liquids, and uncommon magnetic orders [1]. In real materials, the zigzag (Na₂IrO₃ [5] and $4d$ TMOs α -RuCl₃ [6–8]), spiral (Li₂IrO₃ [9–11]) type magnetic orderings, and a canted antiferromagnetic (AF) structure (Sr₂IrO₄) [12,13] have been found.

Generally, to study spin dynamics in a spin-1/2 system with a magnetically ordered ground state and small quantum

fluctuations, the famous SU(2) linear spin-wave theory [14] are used, in which the spin is regarded as a classical three-component vector and its fluctuations are described by rotations of the vector. However, quantum spin systems in fact exhibit richer orderings, and multipolar orderings may emerge when both the spin and orbital degrees of freedom are involved [15]. Spin-orbital Mott insulators intrinsically involve the spin and orbital degrees of freedom, so a nontrivial multipolar nature will be resulted from the SOC [1,16,17]. Of course, the effectiveness of the multipolar exchange interactions depends on the strength of the SOC. If the mixing between the $J_{\text{eff}} = 3/2$ and $J_{\text{eff}} = 1/2$ states is vanishingly small, the low-energy physics is essentially described by the $J_{\text{eff}} = 1/2$ Kramers doublet, such as that in the $5d^5$ configuration of Na₂IrO₃ and Li₂IrO₃. In this case, the Kramers doublet effectively behaves as a pseudo spin-1/2 and the resulting spin-exchange model can be obtained by projecting the electronic Hamiltonian onto the $J_{\text{eff}} = 1/2$ Kramers doublet. Therefore one can resort to the SU(2) linear spin-wave theory [14] to study the low-energy excitations of a magnetically ordered ground state in this spin-1/2 system. However, in other SOC cases where the effective $J_{\text{eff}} = 1/2$ picture breaks down or the mixing between the $J_{\text{eff}} = 3/2$ and $J_{\text{eff}} = 1/2$ states is appreciable, the multipolar exchange interactions will play an important role in their spin dynamics. Thus it is insufficient to treat the local states as the rotations of a classical three-component angular momentum, and a generalization of the SU(2) to SU(N) ($N > 2$) spin-wave theory is needed [18]. On the other hand, even in the case that the $J_{\text{eff}} = 1/2$ picture is applied, one will also need to carry out the calculation by SU(N) spin-wave theory when studying both the low-energy spin excitations within the $J_{\text{eff}} = 1/2$ states and those resulting from spin flippings across the $J_{\text{eff}} = 1/2$ and $J_{\text{eff}} = 3/2$ states, because now the dimension of the local Hilbert space on each site includes more than two spin degrees of freedom.

*jxli@nju.edu.cn

Recently, a unified framework for the $SU(N)$ spin-wave theory based on the multi-boson approach has been introduced [19–22]. In the $SU(N)$ spin-wave theory, N corresponds to the dimension of the local Hilbert space on one site in the fundamental representation of the multi-boson approach. Besides the application in the multipolar spin systems, this multi-boson approach can also be used to describe both the spin and orbital waves, when these two degrees of freedom are separated. In the orbital systems, when the orbitals are ordered like the spins, we can treat the orbital excitations as bosons and calculate the dispersions of orbital waves by the linear spin-wave theory [23–28]. On the other hand, in the presence of SOC, the excitations across the SOC-induced gap could also be regarded as bosonic pseudo-orbital excitations. Since the generators of the $SU(N)$ group can be represented as bilinear forms in N -flavored bosons, instead of two-flavored bosons in the $SU(2)$ spin-wave theory, the low-energy modes of the $SU(N)$ spin-wave theory are described by $(N - 1)$ -flavored bosons and the other flavor denotes the ground state, which would provide a more accurate description of low-energy excitations for unconventional magnetic orders.

In this paper, we will use the $SU(N)$ spin-wave theory to study the magnetic excitations in spin-orbital Mott insulators. In the $SU(N)$ spin-wave theory, the local order parameter is defined in the space of $SU(N)$ unitary transformations of local states, and consists of $N^2 - 1$ components in the most general form. Therefore a universal local mean-field theory facilitating its application is required. Here, we introduce a kind of this general efficient approach based on the supercoherent state [29], which fully includes the on-site quantum fluctuations essential for multipolar states. As an illustration, we first apply the $SU(N)$ spin-wave theory to a toy three-band Hubbard model on a hexagon lattice, and focus on the examination of the effect of Hund's coupling by calculating the weights of $J_{\text{eff}} = 1/2$ states in the ground state and spin-wave spectra. If the SOC is not large enough to lift the spin-orbital excitations, jumping from the $J_{\text{eff}} = 1/2$ to $J_{\text{eff}} = 3/2$ states, apart from the magnons within the $J_{\text{eff}} = 1/2$ doublet, the Hund's coupling would mix the spin-orbital excitations with the magnons. Therefore the low-energy physics is not governed only by the $J_{\text{eff}} = 1/2$ effective Hamiltonian. We then study the spin excitations in two systems of TMOs, α - RuCl_3 , and Sr_2IrO_4 , where the effective Hamiltonian includes both spin and orbital degrees of freedom, by using the $SU(N)$ linear spin-wave theory. Our results for the magnetic ground states and their low-energy spin dynamics in two systems are consistent with recent experiments [3,7,8,13]. In addition, we can obtain the high-energy spin-orbital excitations across the gap in the presence of the spin-orbital coupling.

The paper is organized in the following manner. In Sec. II, we briefly review the Schwinger boson representation, then introduce the general local mean-field method and the $SU(N)$ linear spin-wave theory. In Sec. III, based on the $SU(4)$ antiferromagnetic Hamiltonian [30–32], we calculate the spin-wave excitations and spin-3/2's $l = 2$ multipole-multipole correlation function. In Sec. IV, we apply the $SU(N)$ spin-wave theory to spin-orbital Mott insulators. First, we derive an effective Hamiltonian from a three-band Hubbard model with the SOC in the hexagon lattice and study the magnetic dynamics by the $SU(N)$ spin-wave theory. Then we calculate

the spin correlation function of α - RuCl_3 with the five-band Hubbard model and correlation function of resonant inelastic x-ray scattering (RIXS) operators [33] of Sr_2IrO_4 with a three-band Hubbard model.

II. $SU(N)$ LINEAR SPIN-WAVE THEORY

Muniz *et al.*, present a mathematical framework of the multiboson approach to generalize the traditional spin-wave theory from $SU(2)$ to $SU(N)$ [22]. As we know, the effective exchange models from the electronic models in the strong interaction limit would always be written as

$$H_0 = J_{\mu\nu\mu'\nu'}^{rr'} S_r^{\mu\nu} S_{r'}^{\mu'\nu'} + h_{\mu\nu}^r S_r^{\mu\nu}, \quad (1)$$

where the repeated index $r, r', \mu, \nu, \mu', \nu'$ is summed up, and $S_r^{\mu\nu}$ are the generators of $SU(N)$ group, which obey the commutation relations

$$[S_r^{\mu\nu}, S_{r'}^{\mu'\nu'}] = \delta_{r,r'} (S_r^{\mu\nu'} \delta_{\mu\nu} - S_r^{\mu'\nu} \delta_{\mu\nu'}). \quad (2)$$

These spin operators can be represented by Schwinger bosons. In the spin-wave theory, one of the flavors will be condensed depending on a given magnetic order and the rest $N - 1$ flavors are used to describe the low-energy modes of the system. In this section, we will first review the multi-boson approach based on the Schwinger boson representation. Then, a general local mean-field method will be introduced and applied to the $SU(N)$ linear spin-wave theory.

A. Schwinger boson representation

It is often useful to map a spin model into a bosonic one, which may be easier to study since bosons have simple commutation relations. Also, the common magnons are bosonic excitations which are proper to be represented in bosonic language. In the Schwinger boson representation, the $SU(N)$ generators are written as [34]

$$S_r^{\mu\nu} = b_r^{\mu\dagger} b_r^\nu, \quad (3)$$

$$\sum_{\mu=0}^{N-1} b_r^{\mu\dagger} b_r^\mu = n_b, \quad (4)$$

where $b_r^{\mu\dagger}$ and b_r^μ ($\mu = 0, 1, \dots, N - 1$) are bosonic creation and annihilation operators on the local site r , respectively. Equation (4) is a constraint on the number of bosons in the physical space, and n_b denotes the order of the irreducible representations of $SU(N)$ group. Here we use the fundamental representation $n_b = 1$ for simplicity. Thus N indicates the dimensions of the local state and there is an one-to-one correspondence between each flavor and each local dimension. When $n_b \neq 1$, the spin-wave theory extends to high irreducible representations of $SU(N)$ [35]. For the well-known $SU(2)$ linear spin-wave theory, we can set $n_b = 2S$ for the spin- S systems. Furthermore, the space of local operators is a N^2 -dimensional linear space, which could be expanded on the basis of the identity and the $N^2 - 1$ generators of $SU(N)$ group. Correspondingly, the identity can be represented by the particle number operator and $N^2 - 1$ generators can be expressed by bilinear forms $b^{\mu\dagger} b^\nu$. So, any local operator can be expressed as a linear combination of bosonic bilinear forms.

To sum up, all local fluctuations are described by bosonic particle-hole forms $b^{\mu\dagger}b^{\nu}$. For instance, if there is a local spin $S = 3/2$, then local fluctuations can be expanded as the multipole expansion, which has $16 = (2S + 1)^2$ different scattering channels classified by the total spin of a pair of particle and hole,

$$M_{l,m} = \sum_{m_1 s_2 s_1} (-1)^{s_2+m-m_1} C_{m_1, m-m_1, m}^{s_1, s_2, l} b^{s_1, m_1\dagger} b^{s_2, m_1-m}, \quad (5)$$

where $C_{m_1, m-m_1, m}^{s_1, s_2, l}$ are Clebsch-Gordan coefficients, and $(s_1, m_1), (s_2, m - m_1)$ are the spin quantum numbers of the particle and hole, respectively. $M_{l,m}$ are multipole spin operators. $M_{l,m}$ is the particle number operator when $l = 0$, the dipolar operators S_+ , S_- , and S_z when $l = 1$, and the quadrupolar and octupolar operators when $l = 2$ and 3. There are totally $16 = \sum_{l=0}^3 2l + 1$ multipole spin operators, which are equal to the dimension of the space of local operators and can also be expanded by $SU(N)$ generators. Therefore $SU(N)$ spin-wave theory based on this multiboson approach includes all of bosonic multipolar excitations.

B. Local mean-field method

It is necessary to construct a general local mean-field method to utilize all advantages of the $SU(N)$ spin-wave theory. As we known, the parameter manifold of an n -dimensional (n -D) state is the $(n-1)$ -D complex projective space $CP(n-1)$ when the overall phase is neglected. There are $n-1$ complex parameters, which are $2(n-1)$ real parameters. The variational local mean-field state should span all over the space. So, according to the supercoherent states constructed by Fatyga *et al.* [29], we assume that the test local wave function is generated from a unitary transformation acting on an given state,

$$|T\rangle_r = U(\mathbf{x}_r) b_r^{0\dagger} |0\rangle. \quad (6)$$

$U(\mathbf{x}_r)$ is the unitary transformation and $|0\rangle$ is the vacuum without any bosons:

$$U(\mathbf{x}_r) = \exp \left[i \sum_{\mu \neq 0} (x_r^{2\mu-1} (b_r^{0\dagger} b_r^\mu + b_r^{\mu\dagger} b_r^0), \right. \\ \left. + x_r^{2\mu} (i b_r^{\mu\dagger} b_r^0 - i b_r^{0\dagger} b_r^\mu)) \right] \quad (7)$$

$$|0\rangle = \underbrace{(0, 0, 0, \dots, 0)}_n^T, \quad (8)$$

where $\mathbf{x} \in \mathbb{R}^{2(n-1)}$, $2(n-1)$ -D real space. Obviously, $U(\mathbf{x}_r)$ is particle conserved, so the test state complies with the constraint Eq. (4). In fact, it is arduous to find the minimum in the $\mathbb{R}^{2(n-1)}$ space. Alternatively, we will utilize the structure of $CP(n-1)$ to convert the $\mathbf{x} \in \mathbb{R}^{2(n-1)}$ parameter space to the rotation space in the n -D complex space,

$$\begin{aligned} x^1 &= \theta_1 \cos(\theta_2) \cos(\phi_1), \\ x^2 &= \theta_1 \cos(\theta_2) \sin(\phi_1), \\ x^3 &= \theta_1 \sin(\theta_2) \cos(\theta_3) \cos(\phi_2), \\ x^4 &= \theta_1 \sin(\theta_2) \cos(\theta_3) \sin(\phi_2), \\ &\dots, \end{aligned}$$

$$x^{2n-3} = \theta_1 \sin(\theta_2) \dots \sin(\theta_{n-1}) \cos(\phi_{n-1}),$$

$$x^{2(n-1)} = \theta_1 \sin(\theta_2) \dots \sin(\theta_{n-1}) \sin(\phi_{n-1}),$$

$$\theta_j \in \{0, \pi\}, \phi_j \in \{0, 2\pi\}.$$

When $n = 2$, it is the well-known state of spin-1/2, $|T\rangle = (\cos(\theta_1), e^{i\phi_1} \sin(\theta_1))^T$, where (θ_1, ϕ_1) are Euler angles. It corresponds to a rotation in 2-D complex space or 3-D real space.

The mean-field ground state of the system is the direct product state of local wave functions, $|G\rangle = \bigotimes |T\rangle_r$, which would minimize the energy of $\langle G|H|G\rangle$. Due to the translational symmetry of the ground state, generally only the magnetic cell is considered in the spin-wave theory.

C. SU(N) linear spin-wave approximation

It is known that the spin-wave approximation is based on the Holstein-Primakoff (HP) bosons which define the spin-deviation operators. Its generalization can be obtained by extending the HP representation from $SU(2)$ to $SU(N)$ [22]. To obtain the $SU(N)$ HP bosons, we should first determine the condensed flavor which creates the local state minimizing the mean-field energy. According to the variational form of the mean-field ground state introduced in the last subsection, the condensed flavor is the one minimizing $\langle G|H|G\rangle$, with $|G\rangle = \prod_r \tilde{b}_r^{0\dagger} \otimes |0\rangle_r$. It is related to the Schwinger boson \mathbf{b}_r via the unitary transformation Eq. (7),

$$\tilde{b}_r^{0\dagger} = \sum_{\mu} U_{0\mu}(\mathbf{x}_r) b_r^{\mu\dagger}. \quad (9)$$

Namely, $\tilde{b}_r^{0\dagger}$ is the $\mu = 0$ component of $\tilde{\mathbf{b}}_r$, and the corresponding creation and annihilation operators are replaced by a number according to the constraint Eq. (4),

$$\tilde{b}_r^{0\dagger} \simeq \tilde{b}_r^0 \simeq \sqrt{1 - \sum_{\mu=1}^{n-1} \tilde{b}_r^{\mu\dagger} \tilde{b}_r^\mu}. \quad (10)$$

Then, the $N-1$ bosons $\tilde{b}_r^{\mu \neq 0}$ become the HP bosons, which describe the spin waves originating from fluctuations around the ordered spin state created by the condensed flavor $\tilde{b}_r^{0\dagger}$. Substituting Eq. (10) into the Hamiltonian (1) and retaining only the quadratic terms, we get

$$\begin{aligned} H \simeq & \sum_{\langle r, r' \rangle} J_{0000}^{rr'} + (J_{\mu 0 0 \nu}^{rr'} b_r^{\mu\dagger} b_{r'}^{\nu} + J_{0 \nu 0 \nu}^{r, r'} b_r^{\nu} b_{r'}^{\nu} + \text{H.c.}) \\ & + \sum_r h_{00}^r + h_{\mu' \nu'}^r b_r^{\mu' \dagger} b_r^{\nu'} + \sum_{\langle r, r' \rangle} [(J_{\mu \nu 0 0}^{rr'} - J_{0000}^{rr'} \delta_{\mu \nu}) b_r^{\mu\dagger} b_{r'}^{\nu} \\ & + (J_{00 \mu' \nu'}^{rr'} - J_{0000}^{rr'} \delta_{\mu' \nu'}) b_{r'}^{\mu' \dagger} b_r^{\nu'}], \end{aligned} \quad (11)$$

where the index $\mu, \nu, \mu', \nu' \neq 0$ and will be summed up when appear twice in a single term, and the tilde on $J_{\mu \nu \mu' \nu'}^{rr'}$ and b_r^μ , which denotes the expressions after the unitary transformation that minimizes the mean-field variational energy, is omitted for simplicity.

Now Eq. (11) is a quadratic bosonic Hamiltonian and can be solved by performing the Fourier transformation,

$$b_k^\mu = \frac{1}{\sqrt{L}} \sum_r b_r^\mu e^{i\mathbf{k} \cdot \mathbf{r}}, \quad (12)$$

with L the number of the magnetic unit cells. It leads to

$$H = \sum_k \psi_k^\dagger h(k) \psi_k, \\ \psi_k = (b_k^1, \dots, b_k^{M(N-1)}, b_{-k}^{1\dagger}, \dots, b_{-k}^{M(N-1)\dagger})^T, \quad (13)$$

where M is the size of magnetic cell. There are two diagonalization methods for a bosonic Hamiltonian as proposed by White [36] and Colpa [37]. After diagonalization, we get the spin-wave dispersion $\epsilon_\mu(k)$ as expressed by

$$H = \sum_{\mu=1}^{M(N-1)} \epsilon_\mu(k) \gamma_k^{\mu\dagger} \gamma_k^\mu, \\ \gamma_k^\mu = T_{\mu'}^\mu \psi_k^{\mu'}, \quad (14)$$

with $T_{\mu'}^\mu$ the element of the matrix used to diagonalize the Hamiltonian, and $\psi_k^{\mu'}$ the μ th component of ψ_k . As noted, the $SU(N)$ spin-wave theory includes not only the dipole-dipole correlations, but also the multipole-multipole correlations. In general, the correlation function of two $SU(N)$ generators can be written by

$$S^{\mu\nu\mu'\nu'}(k, \omega) = \frac{1}{2M(N-1)} \int dt e^{-i\omega t} \\ \times \sum_{r,r'} e^{i\mathbf{k}\cdot(\mathbf{r}-\mathbf{r}')} \langle S_r^{\mu\nu} S_{r'}^{\mu'\nu'}(t) \rangle. \quad (15)$$

As same as the $SU(2)$ linear spin-wave theory, only the quadratic forms of the dynamical part of correlation functions are calculated. Therefore the correlation function is expanded in $\langle b^{\mu\dagger} b^\mu \rangle$, which describes the probability to excite one of bosonic excitations. It is clear that there are $M(N-1)$ spin-wave modes.

III. $SU(4)$ ANTIFERROMAGNETIC MODEL

We first calculate the spin-wave spectra for the $SU(4)$ antiferromagnetic model in a square lattice to illustrate the application of the $SU(N)$ linear spin-wave theory in tackling multipolar problems. The natural way to reach a $SU(4)$ system is to put electrons with spin-1/2 into a doubly degenerate band giving another $SU(2)$ degree of freedom, though the full symmetry of the model depends on details like hoppings and the Hund's rule coupling. One can also realize this system from the generic one band Hubbard model loaded with spin-3/2 fermions. We note that there is little chance to load spin-3/2 fermions into a single band in condensed matters. Instead, there is possibility in the ultracold atomic systems, which can have spins higher than 1/2 in the lowest hyperfine multiplets [38–40]. As an example, we consider the $SU(4)$ antiferromagnetic model derived from the one-band spin-3/2 fermionic Hubbard model. Due to Paulis exclusion principle, the wave functions of two on-site fermions have to be antisymmetric. The total spin of two on-site spin-3/2 fermions can only be either singlet ($S = 0$) or quintet ($S = 2$). So the effective model at quarter-filling will have only two exchange channels H_s for

$S = 0$ and H_q for $S = 2$,

$$H_{\text{ex}} = H_s + H_q, \\ H_s = \frac{4J_0}{18} \sum_{(i,j)} \left(\mathbf{S}_i \cdot \mathbf{S}_j - \frac{9}{4} \right) \left(\mathbf{S}_i \cdot \mathbf{S}_j + \frac{3}{4} \right) \left(\mathbf{S}_i \cdot \mathbf{S}_j + \frac{11}{4} \right), \\ H_q = \frac{4J_2}{18} \sum_{(i,j)} \left(\mathbf{S}_i \cdot \mathbf{S}_j - \frac{9}{4} \right) \left(\mathbf{S}_i \cdot \mathbf{S}_j + \frac{11}{4} \right) \left(\mathbf{S}_i \cdot \mathbf{S}_j + \frac{15}{4} \right),$$

where \mathbf{S}_i are the spin-3/2 vectors. And the spin singlet channel H_s results in the $SU(4)$ antiferromagnetic Hamiltonian:

$$H_s = J_0 \sum_{(i,j)} \left[\sum_{1 \leq a < b \leq 5} \Gamma_i^{ab} \Gamma_j^{ab} - \sum_{a=1}^5 \Gamma_i^a \Gamma_j^a \right], \quad (16)$$

where Γ^a are Dirac matrices which form Clifford algebra, $\{\Gamma^a, \Gamma^b\} = 2\delta^{ab}$ and $\Gamma^{ab} = [\Gamma^a, \Gamma^b]/(2i)$. Specifically, the five Dirac matrices can be expressed as tensor products of two Pauli matrices ($\sigma^\alpha, \tau^\beta$), or represented by symmetric bilinear combinations of the components of a spin-3/2 operator, S^x, S^y, S^z :

$$\Gamma^1 = \sigma^z \tau^y = \frac{1}{\sqrt{3}} \{S^y, S^z\}, \\ \Gamma^2 = \sigma^z \tau^x = \frac{1}{\sqrt{3}} \{S^x, S^z\}, \\ \Gamma^3 = \sigma^y \tau^0 = \frac{1}{\sqrt{3}} \{S^x, S^y\}, \\ \Gamma^4 = \sigma^x \tau^0 = \frac{1}{\sqrt{3}} [(S^x)^2 - (S^y)^2], \\ \Gamma^5 = \sigma^z \tau^z = (S^z)^2 - \frac{5}{4}.$$

The so-called $SU(4)$ antiferromagnetism comes from the hidden $SU(4)$ symmetry in a bipartite lattice [31]. To recognize this hidden symmetry, we can define a particle-hole transformation $b^\mu \rightarrow \mathcal{J} b^{\mu\dagger}$ with an antisymmetric matrix $\mathcal{J} = i\sigma^x \tau^y$. With this operation, the fundamental representation transforms to a conjugate representation where $\Gamma^{ab*} = \Gamma^{ab}$ and $\Gamma^{a*} = -\Gamma^a$. If transforming all B sublattices into the conjugate representation, then we have

$$H_s = J_0 \sum_{(i,j)} \left[\sum_{1 \leq a < b \leq 5} \Gamma_i^{ab*} \Gamma_j^{ab} + \sum_{a=1}^5 \Gamma_i^{a*} \Gamma_j^a \right]. \quad (17)$$

It is apparent that Eq. (17) is invariant under $SU(4)$ rotations and the conjugate rotations on sublattices A and B , which is hidden in Eq. (16). Also, all 15 Γ operators together span the $SU(4)$ algebra. Among them, the 10 Γ^{ab} operators are $SO(5)$ antisymmetric tensors, while the five Γ^a are $SO(5)$ vectors. Thus the Hamiltonian (16) obviously possesses $SO(5)$ symmetry.

To use the $SU(4)$ linear spin-wave theory, we expand the Dirac matrices by the $SU(N)$ generators and write them in the Schwinger boson representation:

$$\Gamma^a = \sum_{\sigma\sigma'} b^{\sigma\dagger} \Gamma_{\sigma\sigma'}^a b^{\sigma'}, \quad (18)$$

where $\Gamma_{\sigma\sigma'}^a$ are elements of Dirac matrices Γ^a . Then, the $SU(4)$ antiferromagnetic Hamiltonian Eq. (16) can be represented

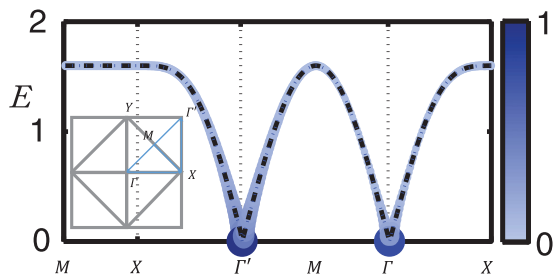


FIG. 1. Spin waves of the SU(4) antiferromagnetic model in a square lattice along high symmetry directions. The dashed lines denote the dispersions, and the size and color of marks indicate the intensity of quadrupolar-quadrupolar correlation functions.

by the four-flavor bosons b^σ . As introduced in Sec. II B, the variational local mean-field wave functions are related to the SU(4) transformation with six parameters $(\theta_i^1, \theta_i^2, \theta_i^3, \phi_i^1, \phi_i^2, \phi_i^3)$. Thus if we consider a four-site variational wave functions, there are 24 parameters in total. Varying these parameters to minimize the mean-field energy, we would get the local mean-field wave functions of the ground state. The results suggest that the ground state of Hamiltonian (16) has a long-range Neel order, which is consistent with quantum Monte Carlo simulations [41]. For this magnetic ordered state, we can choose the quantization direction with three order parameters: $(\Gamma^{12}, \Gamma^{34}, \Gamma^5) = ((-1)^{x+y}m, (-1)^{x+y}m, m)$. In the numerical calculation, the local mean-field wave functions are given as $(1, 0, 0, 0)^T$ for A sublattices and $(0, 0, 0, 1)^T$ for B sublattices. It is easy to check that the order parameters satisfy the SU(4) antiferromagnetic order. As introduced in Sec. II, after identifying the condensed flavor according to the local mean-field wave functions, we can get a free bosonic Hamiltonian by retaining only the quadratic terms of boson operators, and then calculate the dispersion of spin waves by diagonalizing the resulting Hamiltonian.

In the case of spin-3/2, the order parameters can be expanded in multipole orders as defined in Eq. (5):

$$\Gamma^{12} = \frac{2}{\sqrt{5}}(2M_{1,0} - M_{3,0}),$$

$$\Gamma^{34} = \frac{2}{\sqrt{5}}(M_{1,0} + 2M_{3,0}),$$

$$\Gamma^5 = 2M_{2,0}.$$

Therefore we choose to calculate a quadrupolar-quadrupolar correlation function,

$$M_2(k, \omega) = \sum_{r, r'} e^{ik \cdot (r-r')} \int dt e^{-i\omega t} \left\langle \sum_m M_{2,m}(\mathbf{r}) M_{2,m}^\dagger(\mathbf{r}, t) \right\rangle,$$

to illustrate the application in multipolar problems. The numerical results of the spin-wave dispersions and correlation function along high symmetry directions are shown in Fig. 1. We find that the spin waves exhibit the same dispersions to those in the SU(2) antiferromagnetic system in a square lattice, as denoted by the dashed lines in Fig. 1. However, the Goldstone manifold is $\text{CP}(3) = \text{U}(4)/[\text{U}(1) \otimes \text{U}(3)]$ with six branches which are degenerate, instead of two branches in the SU(2) case. Moreover, the quadrupolar-quadrupolar

correlation function exhibits a noticeable intensity at the $\Gamma = (0, 0)$ point. It is in sharp contrast to the behavior of the antiferromagnetic spin-spin correlation, which vanishes at that point. The comparable intensity of the correlation function at $\Gamma = (0, 0)$ and $\Gamma' = (\pi, \pi)$ points is a character of the SU(4) antiferromagnetism.

IV. SU(N) SPIN-WAVE STUDY OF TMOS

Theoretically, TMOs are usually described by the multiband Hubbard model, so we will first present a general method to derive the effective exchange model from an electronic model in the strong interaction limit. The multiband Hubbard model is given by

$$H = \sum_{(ij), \alpha\alpha'} t_{\alpha\alpha'}^{ij} c_{i\alpha}^\dagger c_{j\alpha'} + \sum_i H_i.$$

Here, the first term is hopping term with $t_{\alpha\alpha'}^{ij}$ the elements of hopping integrals, and α indicates all local degrees of freedom, such as orbitals and spins. H_i are the local interactions which include the multiband Hubbard terms V_i , spin-orbital couplings Λ_i , and local potential fields W_i ,

$$\begin{aligned} V_i &= U \sum_{i\mu} n_{i\mu\uparrow} n_{i\mu\downarrow} + U' \sum_{i, \mu < \nu} \sum_{\sigma\sigma'} n_{i\mu\sigma} n_{i\nu\sigma'} \\ &+ J \sum_{i, \mu < \nu} \sum_{\sigma\sigma'} c_{i\mu\sigma}^\dagger c_{i\nu\sigma'}^\dagger c_{i\mu\sigma'} c_{i\nu\sigma} \\ &+ J' \sum_{i, \mu < \nu} c_{i\mu\uparrow}^\dagger c_{i\mu\downarrow}^\dagger c_{i\nu\downarrow} c_{i\nu\uparrow}, \end{aligned} \quad (19)$$

$$\Lambda_i = \lambda \sum_{\mu\sigma\mu'\sigma'} \mathbf{S}_{i\sigma\sigma'} \cdot \mathbf{L}_{i\mu\mu'} c_{i\mu\sigma}^\dagger c_{i\mu'\sigma'}, \quad (20)$$

$$W_i = \sum_{\alpha\beta} w_{i\alpha\beta} c_{i\alpha}^\dagger c_{i\beta}, \quad (21)$$

where U (U') is the intraorbital (interorbital) Coulomb interaction, J_h and J' are the Hund's coupling and pair hopping, respectively. \mathbf{S}_i and \mathbf{L}_i are matrix representation of the spin and orbital angular momentum vectors, respectively. In this paper, we employ $U = U' + 2J_h$ and $J' = J_h$ as used usually.

By means of the perturbation theory, we treat the hopping terms as the perturbation in the strong interaction limit and obtain the effective exchange model, which can be generally written as

$$H_{\text{eff}} = \sum_i P_i^0 H_i P_i^0 + \sum_{(i,j)} [H_{i \rightarrow j} + H_{j \rightarrow i}], \quad (22)$$

$$H_{i \rightarrow j} = \sum_{\substack{(lre) \\ \alpha\alpha'\beta\beta}} \frac{1}{\Delta_{lre}} t_{\alpha\alpha'}^{(ij)} [s_i^{\alpha\beta}]_{(lre)} t_{\beta\beta'}^{(ji)} [\tilde{s}_j^{\beta\alpha}]_{(lre)}. \quad (23)$$

The first term in Eq. (22) is the zero-order perturbation term, and the second is the second-order perturbation term accounting for the virtual hoppings of electrons contributing to spin exchanges. P_i^0 is the operator projecting the Hamiltonian H_i into its low-energy subspace. $s_i^{\alpha\beta} = c_{i\alpha}^\dagger c_{i\beta}$ and $\tilde{s}_j^{\beta\alpha} = c_{j\alpha} c_{j\beta}^\dagger$ are SU(N) generators and their conjugate representations, respectively. (lre) denotes various exchange channels related to the virtual processes from a low-energy state $|r_i\rangle \otimes |r_j\rangle$ to

a high one $|e_i\rangle \otimes |e_j\rangle$, and back to the low one $|l_i\rangle \otimes |l_j\rangle$, where $|r_i\rangle$, $|e_i\rangle$, and $|l_i\rangle$ are the eigenstates of Hamiltonian H_i . Taking the half-filling one-band Hubbard model as an example, when one particle hops from j site to i , the intermediate states $|e_i\rangle$ and $|e_j\rangle$ become doubly-occupied and vacuum states, respectively, while the low-energy states $|m_{i(j)}\rangle$ ($m = l, r$) are singly-occupied states. $1/\Delta_{lre} = 1/2(E_{li} + E_{lj} - E_{ei} - E_{ej}) + 1/2(E_{ri} + E_{rj} - E_{ei} - E_{ej})$, in which E_{mi} ($m = l, e, r$) is the eigenenergy of the local state $|m_i\rangle$ on the site i . $[\cdot]_{(lre)}$ indicates a special representation of $s_i^{\alpha\beta}$ and $\tilde{s}_j^{\beta\alpha}$ in the states $(|l_i\rangle, |r_i\rangle, |e_i\rangle, |l_j\rangle, |r_j\rangle, |e_j\rangle)$,

$$\begin{aligned} [s_i^{\alpha\beta}]_{(lre)} &= |l_i\rangle\langle l_i|c_i^{\alpha\dagger}|e_i\rangle\langle e_i|c_i^\beta|r_i\rangle\langle r_i|, \\ &= \langle l_i|c_i^{\alpha\dagger}|e_i\rangle\langle e_i|c_i^\beta|r_i\rangle S_i^{l_r i}, \\ [\tilde{s}_j^{\beta\alpha}]_{(lre)} &= |l_j\rangle\langle l_j|c_j^\alpha|e_j\rangle\langle e_j|c_j^{\beta\dagger}|r_j\rangle\langle r_j|, \\ &= \langle l_j|c_j^\alpha|e_j\rangle\langle e_j|c_j^{\beta\dagger}|r_j\rangle S_j^{l_r j}, \end{aligned}$$

where $S_i^{l_r i} = |l_i\rangle\langle r_i|$ is the $SU(N)$ generator in the fundamental representation defined in the low-energy space of H_i . We note the symmetry of Hamiltonian (23) is related to the symmetry of $(|l_i\rangle, |r_i\rangle, |e_i\rangle)$ and $t_{\alpha'\alpha}^{ij}$, which are determined by the symmetry of the crystal structure. Now with Eq. (22), we will carry out the $SU(N)$ spin-wave calculation.

A. Three-band Hubbard model with an SOC on the hexagon lattice

In this section, we consider a simple three-band Hubbard model with one spin-1/2 particle per site and SOC on a hexagon lattice. The Hubbard term preserves the $SU(2)$ and $SO(3)$ symmetry with $U = U' + 2J_h$. Focusing on the effect of Hund's coupling and SOC, we suppose a simply isotropic hopping term, $t_{\alpha'\alpha}^{ij} = t\delta_{\alpha'\alpha}$ only among the nearest neighbors.

If SOC is absent, its effective exchange model is comparatively explicit. Due to the three degenerated energy bands, the low-energy states $|r_i\rangle$ ($|l_i\rangle$) are sixfold degenerated singly-occupied states with zero energy. The intermediate state $|e_i\rangle \otimes |e_j\rangle$ is a direct product of a vacuum state on one site and a doubly occupied state on the other site. Because the wave functions of two on-site fermions have to be antisymmetric, there are only three kinds of doubly occupied states, which are (1) ninefold degeneracy with total spins $S = 1$, total orbital momentums $L = 1$ and $\Delta_{lre} = -U + 3J_h$, (2) fivefold degeneracy with total spins $S = 0$, total orbital momentums $L = 2$ and $\Delta_{lre} = -U + J_h$, and (3) nondegeneracy with total spins $S = 0$, total orbital momentums $L = 0$ and $\Delta_{lre} = -U - 2J_h$. The local wave function $|m_i\rangle$ can be written according to the quantum numbers or the results of numerical calculations.

When SOC is comparable to the Hubbard term, $\lambda \sim U$, there will be $80 = 4 \times 5 \times 4$ kinds of channels due to the interplay of the SOC and Hund's coupling: two kinds of $|r_i\rangle$ or $|l_i\rangle$ with energy $\lambda/2$ and $-\lambda$, respectively, and five kinds of $|e_i\rangle$ with energy $U - 3J_h - \lambda/2, (2U - J_h - \lambda \pm \sqrt{25J_h^2 + 10J_h\lambda + 9\lambda^2})/2$ and $(4U - 8J_h + \lambda \pm \sqrt{16J_h^2 + 8J_h\lambda + 9\lambda^2})/4$. We can diagonalize the local Hamiltonian H_i to get these wave functions $(|l_i\rangle, |r_i\rangle, |e_i\rangle)$ and the

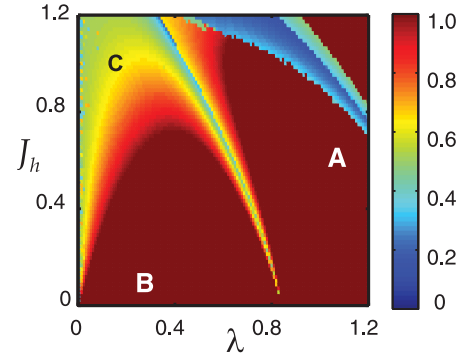


FIG. 2. Weights of the $J_{\text{eff}} = 1/2$ states in ground states vary with λ and J_h , calculated based on the three band Hubbard model with an SOC on the hexagon lattice. The intraorbital Coulomb interaction is $U = 5.0$.

corresponding energies. Then substituting them into Eq. (22), we can obtain the exchange model.

If $J_h = 0, \lambda = 0$, H_i has $SU(6)$ symmetry, so does the eigenstates $(|l_i\rangle, |r_i\rangle, |e_i\rangle)$, but the symmetry of eigenstates will be broken into $SU(2)$ by either SOC or Hund's coupling. Furthermore, when $t_{\alpha'\alpha}^{ij}$ is $SU(2)$ symmetrical, the effective Hamiltonian must be $SU(2)$ symmetrical too. If $\lambda \gg J_h$, only the lowest energy channel is active. In this case, the Hamiltonian can be further approximated to be an effective isospin-1/2 model. However, the Hund's coupling will lower the energy of the states with two spins parallelling, while the SOC will decrease the energy of $J_{\text{eff}} = 1/2$ single-particle states. This would influence the validity of the isospin $J_{\text{eff}} = 1/2$ picture. Therefore we will take both λ and J_h into account to examine the spin-wave spectra of the system.

Using the local mean-field method, we find the ground state consists of a magnetic cell with two sites. Therefore we choose the local mean-field wave functions defined as $|T_A\rangle$ and $|T_B\rangle$ for the two sublattices. In the strong SOC limit, when Hund's coupling is absent, it is known that $|T_A\rangle = \sqrt{2/3}|1, -1/2\rangle - \sqrt{1/3}|0, 1/2\rangle$ and $|T_B\rangle = -\sqrt{2/3}|-1, 1/2\rangle + \sqrt{1/3}|0, -1/2\rangle$ [where $|l^z, s^z\rangle$ representing the local state of orbital and spin quantum number (l^z, s^z)], which is the Kramers doublet of $J_{\text{eff}} = 1/2$ states. For the other general cases, we calculate local mean-field wave functions by the local mean-field method. In order to verify the validity of the $J_{\text{eff}} = 1/2$ picture, we calculate the weight $(\langle J_{\text{eff}} = 1/2 | T_A \rangle + \langle J_{\text{eff}} = 1/2 | T_B \rangle) / 2$ with the hopping term $t = 1$ as unit and $U = 5.0$. The results as functions of λ and J_h are shown in Fig. 2, which can be roughly divided into three regions: (region A) the ground states are dominated by $J_{\text{eff}} = 1/2$ states; (region B) a hump-typed region with small λ and J_h where ground states are also dominated by $J_{\text{eff}} = 1/2$ states; and (region C) J_h is so large that the ground states are mixed with the $J_{\text{eff}} = 3/2$ states. The blue region on the top indicates the divergence of the second order perturbation, resulting from the fact that the SOC gap is comparable to the Hubbard gap.

Then, we show the limitation of the $SU(N)$ spin wave theory in three extreme cases, and the results are presented in Fig. 3. When $J_h = 0$ and $\lambda = 0$, there are highly degenerated zero energy modes as shown in Fig. 3(a). It indicates that the magnetic order are unstable. In fact, the ground state in this

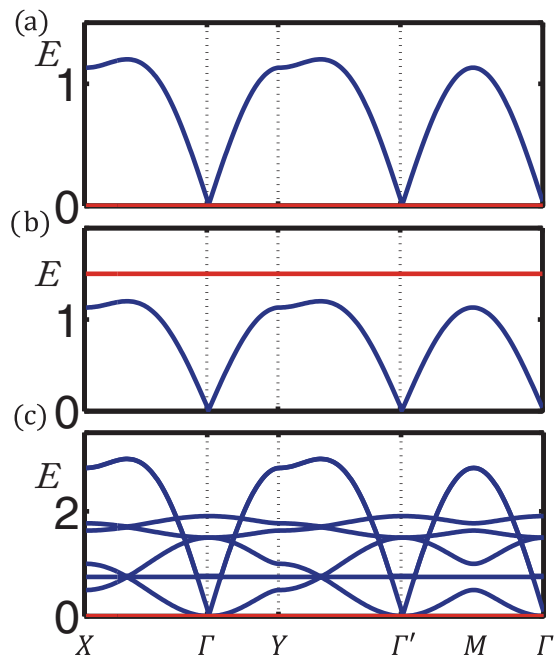


FIG. 3. Spin waves of the three-band Hubbard model on a hexagon lattice with different SOC λ and Hund's coupling J_h . (a) $\lambda = 0.0$, $J_h = 0.0$, (b) $\lambda = 1.0$, $J_h = 0.0$, and (c) $\lambda = 0.0$, $J_h = 1.0$.

situation is the SU(6) plaquette state as shown before [42,43], where SU(6) spins form a local singlet on a hexagon plaquette, so no long-range magnetic order exists. Thus it shows that the SU(N) spin-wave theory can identify this instability. As λ increases, the zero energy modes are lifted [see Fig. 3(b)], and the system approaches ordered phases because the fluctuations become weak gradually as the system deviates from the SU(6) symmetry due to SOC. On the other hand, a ferromagnetic-like spin wave emerges when turning on the Hund's coupling J_h instead of SOC λ . It exhibits a parabolic dispersion around the Γ and Γ' points, as shown in Fig. 3(c). However, there is also some zero energy degeneracies implying an instability of the ground state we used, based on the four-site variational function for the local mean field. We suggest that the ground state may be some kind of resonant-valence-bond states or have a more complicated long-range order. Nevertheless, $\lambda = 0$ is an extreme case, and the spin-wave theory is executable as long as there is a long-range magnetic ordered ground state.

Now, let us study the correlation functions in the three regions A, B, and C, respectively. In the dipole-dipole approximation, the correlation function consists of three parts of contributions: spin flippings within either $J_{\text{eff}} = 1/2$ or $3/2$ states and across the $J_{\text{eff}} = 1/2$ and $J_{\text{eff}} = 3/2$ states, which are denoted by $1 \rightleftharpoons 1$, $3 \rightleftharpoons 3$, and $1 \rightleftharpoons 3$, respectively. In Figs. 4(a)–4(c), we present the dispersions of spin waves denoted by the dashed lines and intensities of correlation functions indicated by the saturation of three different colors and size of markers. The colors will mix as shown by the legend in Fig. 4(e), when spin wave excitations includes more than one type of contributions. In region A, the low-energy spin waves has a linear dispersion around the Γ and Γ' points, and its intensity diverges at the Γ' point while vanishes at the Γ point, suggesting an antiferromagnetic-like spin wave. In

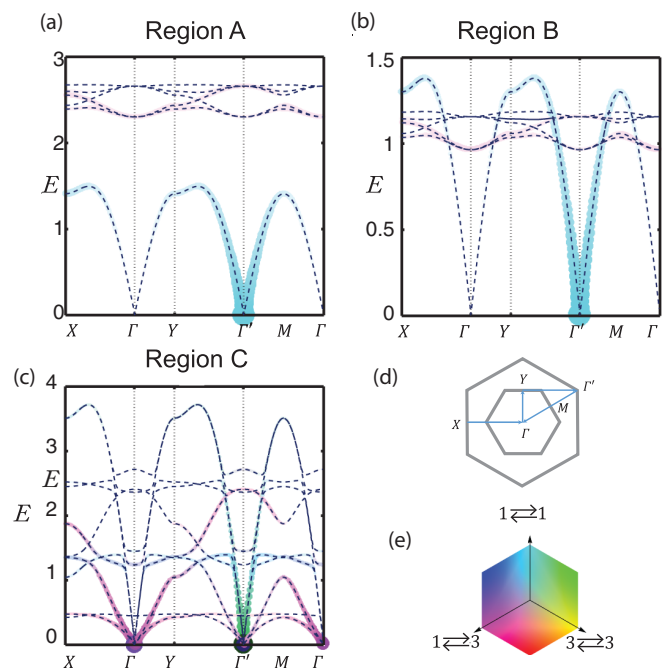


FIG. 4. Spin waves of the three-band Hubbard model on a hexagon lattice with parameters: (a) $\lambda = 0.9$, $J_h = 0.6$, (b) $\lambda = 0.4$, $J_h = 0.4$, and (c) $\lambda = 0.2$, $J_h = 1.1$. The dashed lines denote dispersions. The size and saturation of markers indicate the intensity of the correlation function, and three different channels are indicated by three different colors. (d) Reciprocal lattices and high symmetry directions of a hexagon lattice. (e) The legend indicating the compositions of the correlation function.

the high-energy regime above $2t$, the dispersion is parabolic around the Γ point and the intensity is higher at the Γ point than Γ' point, exhibiting a ferromagnetic-like spin wave. At the meantime, the result calculated by the local mean-field method shows the system has a $J_{\text{eff}} = 1/2$ antiferromagnetic ordered ground state, confirming that the excitations at low energies are indeed antiferromagnetic spin waves. As shown by the cyan-blue color in Fig. 4(a), these low-energy excitations come basically from spin flippings within the $J_{\text{eff}} = 1/2$ states, so the low-energy physics in region A is dominated by isospin-1/2 states. Furthermore, the excitations arising from the spin flippings across the $J_{\text{eff}} = 1/2$ and $J_{\text{eff}} = 3/2$ states as denoted by the magenta color are far beyond the low-energy excitations due to the sufficiently large SOC. Thus we arrive at the conclusion that an effective isospin Heisenberg model can depict the low-energy physics in region A, which is also consistent with the calculation of weights of $J_{\text{eff}} = 1/2$ states in ground states as shown in Fig. 2. When the SOC is decreased, it will enter gradually into region B. In this progress, the gap between the low-energy antiferromagnetic spin waves and the high-energy ferromagnetic spin waves decreases gradually. However, the two spin waves do not entangle as long as J_h is not large enough, although the dispersion of ferromagnetic spin waves overlaps with the low-energy one, as shown in Fig. 4(b) where the colors representing two different kinds of spin waves do not mix. Thus, apart from the effective isospin Heisenberg terms in the Hamiltonian, which describes the antiferromagnetic spin waves, there have to be another term

to describe the ferromagnetic spin waves at least. Starting from region B, one can increase J_h to enter into region C. In this region, the antiferromagnetic and ferromagnetic spin waves are entangled, so that there is no well-defined antiferromagnetic-like spin waves or ferromagnetic-like spin waves, and the local test wave functions of ground state in two different sublattices are not completely orthogonal, namely $\langle T_A | T_B \rangle \approx 0.016$. Because the ground state consists of both $J_{\text{eff}} = 1/2$ and $J_{\text{eff}} = 3/2$ states now, the multipolar orders are inevitable to be taken into account. A direct indication is that an obvious intensity at Γ point now emerges, which is similar to that in the SU(4) antiferromagnetic model as shown in Fig. 1 and is suggestive of emergence of multipolar orders. Thus we examine the ground states by the local mean-field method that the dipolar order parameters $\langle J_{\text{eff}}^\alpha \rangle$ are almost antiferromagnetic, but quadrupolar order parameters $\langle J_{\text{eff}}^\alpha J_{\text{eff}}^\beta + J_{\text{eff}}^\beta J_{\text{eff}}^\alpha \rangle$ are ferromagnetic. In this case, no so-called isospin effective Hamiltonian can be obtained and all degrees of freedom have to be taken into account. So the SU(N) spin-wave theory rather than the traditional SU(2) one should be applicable.

B. α -RuCl₃ and Sr₂IrO₄

In this section, we will use the SU(N) spin-wave theory to study spin dynamics in α -RuCl₃ and Sr₂IrO₄. Both α -RuCl₃ and Sr₂IrO₄ have a d^5 configuration and have an octahedral crystal field. Their differences are that the active electrons residing in $4d$ orbitals of Ru has a smaller SOC than that in $5d$ of Ir, and α -RuCl₃ is a honeycomb lattice while Sr₂IrO₄ is a square lattice.

α -RuCl₃ has a layered crystal structure with Ru³⁺ forming honeycomb lattice layers and the energy bands near the Fermi level are dominated by the d orbitals of Ru³⁺. We consider a five-band Hubbard model with five electrons per site and the on-site crystal field. The tight-binding parameters include the nearest-, next-nearest-, and third-nearest-neighbour hopping integrals, which are obtained by fitting the energy-band dispersions calculated by the first principle calculations and given in our previous paper Ref. [44]. We take $U = 2.7$ eV, $J_h = 0.13U$, $U' = U - 2J_h$, and $\lambda = 0.14$ eV [7,44–48] in the following calculations. Then, an effective exchange model is obtained numerically according to Eq. (22). Due to the large crystal field potential on the e_g orbitals, there are isolated six lowest energy states, onto which we will project the initial and final states. Using the local mean-field method and the SU(6) linear spin-wave approximation introduced in Sec. II, we investigate numerically the magnetic ground state and spin dynamics. The results show that the magnetic ground state has a zigzag-type order of which the magnetic unit cell contains four sites (two cells), in agreement with experiments in α -RuCl₃ [6–8]. The spin-spin correlation functions calculated by Eq. (15) are shown in Fig. 5(a). Below 10 meV, four zigzag spin waves are evident, and the other sixteen excitations above 200 meV come from the spin-orbital excitations across the $J_{\text{eff}} = 1/2$ and $3/2$ states. The low-energy spin waves have a gap about 2 meV at M point and the spin-spin correlation function has a maximum magnitude also at M point. These results are consistent with the recent experiments of inelastic neutron scatterings on α -RuCl₃ [7,8]. On the other hand, the gap between

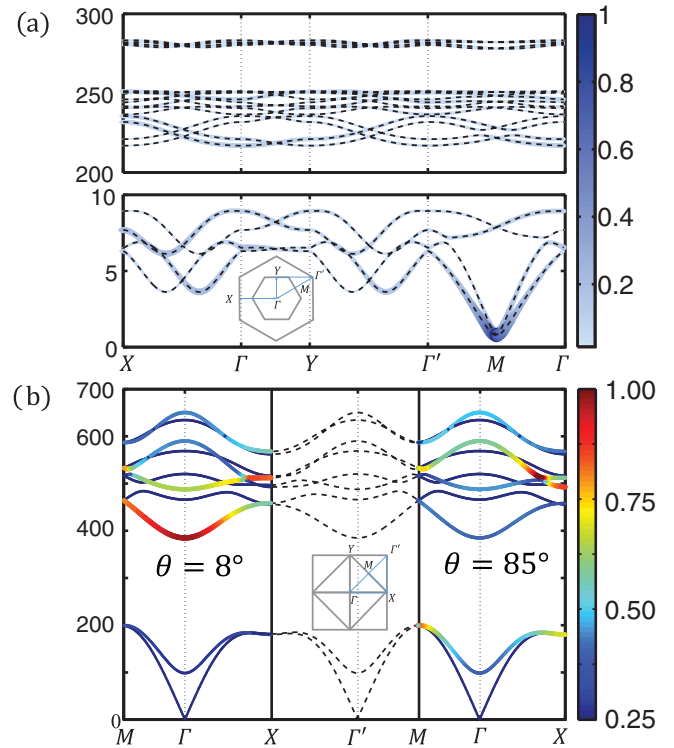


FIG. 5. Spin-spin correlation functions for (a) α -RuCl₃, and correlation functions of RIXS operators [33] for (b) Sr₂IrO₄ along the high-symmetry lines, calculated by the SU(6) spin-wave theory. At the antiferromagnetic wave vector Γ' point, the intensity of the correlation function diverges, so we only plot the dispersion around the Γ' point in (b).

the zigzag spin waves and the spin-orbital excitations is about 210 meV, thus it is suggested that the low-energy physics of α -RuCl₃ could be captured by an effective isospin-1/2 model. We notice that the spin-orbital excitations above 200 meV can only be captured by the SU(6) spin-wave theory, and their features wait for a comparison with future experiments.

Now let us turn to Sr₂IrO₄. We start our investigations from a three-band Hubbard model with a single hole per site to fit the band dispersion around the Fermi level [49,50], and choose $U = 3.6$ eV, $J_h = 0.18U$, and $\lambda = 0.37$ eV [49,50] in the calculation. Because iridium is a strong absorber of neutrons, it is more useful to calculate the resonant inelastic x-ray scattering (RIXS) spectra for the purpose of a comparison with experiments. RIXS involves a second-order process that includes an absorption and an emission of a photon. In the fast collision approximation, the direct RIXS spectrum is proportional to the correlation function of spin-orbital moment operators [33]. Due to the two scattering progresses (absorption and emission), the total angular momentum of spin-orbital moment operators is equal to the coupling of two $l = 1$ angular momenta (angular momentum exchange of the two scatterings is one in the dipole limit). Thus there exist multipole-multipole correlations in RIXS besides the usual dipole-dipole correlations. It is known that the RIXS spectrum of Sr₂IrO₄ is dependent on the incident angle [3]. So, we calculate the correlation function for two different incident angles $\theta = 8^\circ$ and 85° , and the results are presented

in Fig. 5(b) where the left-hand one is for $\theta = 8^\circ$ and the right-hand for $\theta = 85^\circ$. Below 200 meV, the results exhibit gapless antiferromagnetic spin waves dispersing up linearly from the Γ and Γ' points, which are consistent with experiments in Sr_2IrO_4 [3,12,13]. Above 200 meV, a gap of 180 meV exists arising from the SOC, and the spin-orbital excitations across the gap are ferromagnetic-like spin waves that are parabolic around Γ point. Moreover, there is a small gap in the spectra of spin-orbital excitations resulting from the splitting in t_{2g} orbitals. This splitting arises from the tilt of the oxygen octahedron, which is reflected in the tight-binding parameters here. As for the incident-angle dependence of spectra, one can see that the scattering intensity of the low-energy $J_{\text{eff}} = 1/2$ antiferromagnetic magnon is suppressed heavily, and at the same time the spin-orbital excitations are strongly enhanced for a small incident angle such as $\theta = 8^\circ$, as shown in the left-hand side in Fig. 5(b), while an opposite behavior of the spectra is observed for a large incident angle such as $\theta = 85^\circ$ [the right-hand side in Fig. 5(b)]. This dependence is also in agreement with experiments [3].

The results presented above demonstrate a good performance of the SU(N) spin-wave theory in the study of magnetic orders and dynamics in TMOs. Compared with the SU(2) spin-wave theory, the SU(N) theory contains more than one type of uncondensed bosons, so that the spin-orbital excitations and multipolar orders can be described. Of course, the linear approximation used here involves only single particle excitations and does not take their interactions into account. So, the broadening and renormalization of spin-wave spectra are not captured. In this case, the spin-orbital excitations can be regarded as orbital waves excited from the $J_{\text{eff}} = 1/2$ orbital to the $J_{\text{eff}} = 3/2$ orbital, so the ground state looks like a ferro-orbitally ordered state. Therefore the high-energy spin-orbital excitations appear like ferromagnetic spin waves as shown in Fig. 5(b) for Sr_2IrO_4 . However, the interactions between bosons will couple spin-orbital excitations to low-energy antiferromagnetic magnons, so a description other than the spin-wave theory is needed [51,52]. In fact, as shown in Refs. [3,13], the theoretical analysis about the spin-orbital excitations in Sr_2IrO_4 provided a better agreement with the experiment when taking the interactions into account by the self-consistent Born approximation. In addition, to study other spin dynamics, such as magnon decay effects [53,54], one should go beyond the linear order approximation. We note that some modifications of the spin-wave theory [55,56] have been developed in the SU(2) case, their generalizations to the SU(N) case deserve further study.

V. CONCLUSION

In summary, we implement the application of the SU(N) spin-wave theory by introducing an efficient local mean-field

method based on the supercoherent state. The approach is tested firstly by applying it to the investigation of magnetic properties of the SU(4) antiferromagnetic model in a square lattice. Based on the local mean-field method, we find a long-range Neel order, which is consistent with the quantum Monte Carlo simulations, and this order can be interpreted by multipolar orders of 3/2 spins. By calculating the multipolar spin waves of the SU(4) antiferromagnetic model, we find that the distribution of intensity of the quadrupolar-quadrupolar correlation function is similar to that of antiferromagnetic spin-spin correlation in the SU(2) case, except the intensity at the Γ point where a noticeable intensity exist in the SU(4) case. Thus we demonstrate the application of the SU(N) spin-wave theory to the investigation of multipolar orderings. Due to the entanglement of spin and orbital degrees of freedom, the multipole-multipole exchange terms are also present in the effective exchange models of spin-orbital Mott insulators. Only if the spin-orbital coupling is large enough that the low-energy physics is confined in the Kramers doublet, the effective Hamiltonian will be described as an isospin-1/2 model. In this aspect, we examine a toy three-band Hubbard model on a hexagon lattice based on the SU(6) spin-wave theory, which allows us to capture the contributions from the $J_{\text{eff}} = 3/2$ states. We therefore discuss the validity of the isospin-1/2 picture according to weights of $J_{\text{eff}} = 1/2$ states in the ground state and the dipole-dipole correlation function. We find that a noticeable intensity in the excitation spectrum occurs at Γ point when the isospin-1/2 picture becomes invalid due to the Hund's coupling, which is suggestive of the multipolar ordered ground state. Our results demonstrate that the SU(N) spin-wave theory is a more general method for spin-orbital systems.

Finally, we apply the SU(N) spin-wave theory to two $5d^5$ systems of spin-orbital Mott insulators, $\alpha\text{-RuCl}_3$ and Sr_2IrO_4 . Our results for the magnetic ground states and their low-energy spin dynamics in both systems are consistent with recent experiments. The SU(N) spin-wave calculations also provide the spectra for high-energy spin-orbital excitations, which will be helpful for the future experimental investigations. On the other hand, for $5d^1$ systems, which have the higher-rank multipole degrees of freedom [16,57,58], the application of SU(N) spin-wave theory will be an interesting perspective.

ACKNOWLEDGMENTS

This work was supported by the National Natural Science Foundation of China (Grants No. 11374138 and No. 11774152) and National Key Projects for Research and Development of China (Grant No. 2016YFA0300401). W.W. was also supported by the program B for Outstanding Ph.D. candidate of Nanjing University.

- [1] W. Witczak-Krempa, G. Chen, Y. B. Kim, and L. Balents, *Annu. Rev. Condens. Matter Phys.* **5**, 57 (2014).
 [2] B. J. Kim, H. Jin, S. J. Moon, J.-Y. Kim, B.-G. Park, C. S. Leem, J. Yu, T. W. Noh, C. Kim, S.-J. Oh, J.-H. Park, V.

Durairaj, G. Cao, and E. Rotenberg, *Phys. Rev. Lett.* **101**, 076402 (2008).

- [3] J. Kim, M. Daghofer, A. H. Said, T. Gog, J. van den Brink, G. Khaliullin, and B. J. Kim, *Nat. Commun.* **5**, 4453 (2014).

- [4] G. Jackeli and G. Khaliullin, *Phys. Rev. Lett.* **102**, 017205 (2009).
- [5] X. Liu, T. Berlijn, W.-G. Yin, W. Ku, A. Tsvelik, Y.-J. Kim, H. Gretarsson, Y. Singh, P. Gegenwart, and J. P. Hill, *Phys. Rev. B* **83**, 220403 (2011).
- [6] J. A. Sears, M. Songvilay, K. W. Plumb, J. P. Clancy, Y. Qiu, Y. Zhao, D. Parshall, and Y.-J. Kim, *Phys. Rev. B* **91**, 144420 (2015).
- [7] A. Banerjee, J. Yan, J. Knolle, C. A. Bridges, M. B. Stone, M. D. Lumsden, D. G. Mandrus, D. A. Tennant, R. Moessner, and S. E. Nagler, *Science* **356**, 1055 (2017).
- [8] K. Ran, J. Wang, W. Wang, Z.-Y. Dong, X. Ren, S. Bao, S. Li, Z. Ma, Y. Gan, Y. Zhang, J. T. Park, G. Deng, S. Danilkin, S.-L. Yu, J.-X. Li, and J. Wen, *Phys. Rev. Lett.* **118**, 107203 (2017).
- [9] A. Biffin, R. D. Johnson, I. Kimchi, R. Morris, A. Bombardi, J. G. Analytis, A. Vishwanath, and R. Coldea, *Phys. Rev. Lett.* **113**, 197201 (2014).
- [10] S. C. Williams, R. D. Johnson, F. Freund, S. Choi, A. Jesche, I. Kimchi, S. Manni, A. Bombardi, P. Manuel, P. Gegenwart, and R. Coldea, *Phys. Rev. B* **93**, 195158 (2016).
- [11] A. Biffin, R. D. Johnson, S. Choi, F. Freund, S. Manni, A. Bombardi, P. Manuel, P. Gegenwart, and R. Coldea, *Phys. Rev. B* **90**, 205116 (2014).
- [12] B. J. Kim, H. Ohsumi, T. Komesu, S. Sakai, T. Morita, H. Takagi, and T. Arima, *Science* **323**, 1329 (2009).
- [13] J. Kim, D. Casa, M. H. Upton, T. Gog, Y.-J. Kim, J. F. Mitchell, M. van Veenendaal, M. Daghofer, J. van den Brink, G. Khaliullin, and B. J. Kim, *Phys. Rev. Lett.* **108**, 177003 (2012).
- [14] J. T. Haraldsen and R. S. Fishman, *J. Phys.: Condens. Matter* **21**, 216001 (2009).
- [15] P. Santini, S. Carretta, G. Amoretti, R. Caciuffo, N. Magnani, and G. H. Lander, *Rev. Mod. Phys.* **81**, 807 (2009).
- [16] G. Chen, R. Pereira, and L. Balents, *Phys. Rev. B* **82**, 174440 (2010).
- [17] G. Chen and L. Balents, *Phys. Rev. B* **84**, 094420 (2011).
- [18] A. Joshi, M. Ma, F. Mila, D. N. Shi, and F. C. Zhang, *Phys. Rev. B* **60**, 6584 (1999).
- [19] B. Bauer, P. Corboz, A. M. Läuchli, L. Messio, K. Penc, M. Troyer, and F. Mila, *Phys. Rev. B* **85**, 125116 (2012).
- [20] K. Penc, J. Romhányi, T. Rößler, U. Nagel, Á. Antal, T. Fehér, A. Jánossy, H. Engelkamp, H. Murakawa, Y. Tokura, D. Szaller, S. Bordács, and I. Kézsmárki, *Phys. Rev. Lett.* **108**, 257203 (2012).
- [21] J. Romhányi and K. Penc, *Phys. Rev. B* **86**, 174428 (2012).
- [22] R. A. Muniz, Y. Kato, and C. D. Batista, *Prog. Theor. Exp. Phys.* **2014**, 83101 (2014).
- [23] G. Khaliullin and V. Oudovenko, *Phys. Rev. B* **56**, R14243(R) (1997).
- [24] J. van den Brink, W. Stekelenburg, D. I. Khomskii, G. A. Sawatzky, and K. I. Kugel, *Phys. Rev. B* **58**, 10276 (1998).
- [25] J. van den Brink, P. Horsch, F. Mack, and A. M. Oleś, *Phys. Rev. B* **59**, 6795 (1999).
- [26] H. Kusunose and Y. Kuramoto, *J. Phys. Soc. Jpn.* **70**, 3076 (2001).
- [27] S. Ishihara, *Phys. Rev. B* **69**, 075118 (2004).
- [28] E. Saitoh, S. Okamoto, K. Takahashi, K. Tobe, K. Yamamoto, T. Kimura, S. Ishihara, S. Maekawa, and Y. Tokura, *Nature (London)* **410**, 180 (2001).
- [29] B. W. Falyga, V. A. Kostecký, M. M. Nieto, and D. R. Truax, *Phys. Rev. D* **43**, 1403 (1991).
- [30] Y. Qi and C. Xu, *Phys. Rev. B* **78**, 014410 (2008).
- [31] C. Wu, J.-P. Hu, and S.-C. Zhang, *Phys. Rev. Lett.* **91**, 186402 (2003).
- [32] H.-H. Hung, Y. Wang, and C. Wu, *Phys. Rev. B* **84**, 054406 (2011).
- [33] J. Luo, G. T. Trammell, and J. P. Hannon, *Phys. Rev. Lett.* **71**, 287 (1993).
- [34] D. P. Arovas and A. Auerbach, *Phys. Rev. B* **38**, 316 (1988).
- [35] F. H. Kim, K. Penc, P. Nataf, and F. Mila, *Phys. Rev. B* **96**, 205142 (2017).
- [36] R. M. White, M. Sparks, and I. Ortenburger, *Phys. Rev.* **139**, A450 (1965).
- [37] J. Colpa, *Physica A (Amsterdam)* **93**, 327 (1978).
- [38] G. Modugno, F. Ferlaino, R. Heidemann, G. Roati, and M. Inguscio, *Phys. Rev. A* **68**, 011601 (2003).
- [39] T.-L. Ho and S. Yip, *Phys. Rev. Lett.* **82**, 247 (1999).
- [40] S.-K. Yip and T.-L. Ho, *Phys. Rev. A* **59**, 4653 (1999).
- [41] K. Harada, N. Kawashima, and M. Troyer, *Phys. Rev. Lett.* **90**, 117203 (2003).
- [42] P. Nataf, M. Lajkó, P. Corboz, A. M. Läuchli, K. Penc, and F. Mila, *Phys. Rev. B* **93**, 201113 (2016).
- [43] H. H. Zhao, C. Xu, Q. N. Chen, Z. C. Wei, M. P. Qin, G. M. Zhang, and T. Xiang, *Phys. Rev. B* **85**, 134416 (2012).
- [44] W. Wang, Z.-Y. Dong, S.-L. Yu, and J.-X. Li, *Phys. Rev. B* **96**, 115103 (2017).
- [45] A. Koitzsch, C. Habenicht, E. Müller, M. Knupfer, B. Büchner, H. C. Kandpal, J. van den Brink, D. Nowak, A. Isaeva, and T. Doert, *Phys. Rev. Lett.* **117**, 126403 (2016).
- [46] L. J. Sandilands, Y. Tian, A. A. Reijnders, H.-S. Kim, K. W. Plumb, Y.-J. Kim, H.-Y. Kee, and K. S. Burch, *Phys. Rev. B* **93**, 075144 (2016).
- [47] S. M. Winter, Y. Li, H. O. Jeschke, and R. Valentí, *Phys. Rev. B* **93**, 214431 (2016).
- [48] H.-S. Kim, V. V. Shankar, A. Catuneanu, and H.-Y. Kee, *Phys. Rev. B* **91**, 241110(R) (2015).
- [49] H. Watanabe, T. Shirakawa, and S. Yunoki, *Phys. Rev. Lett.* **105**, 216410 (2010).
- [50] H. Wang, S.-L. Yu, and J.-X. Li, *Phys. Rev. B* **91**, 165138 (2015).
- [51] K. Wohlfeld, M. Daghofer, S. Nishimoto, G. Khaliullin, and J. van den Brink, *Phys. Rev. Lett.* **107**, 147201 (2011).
- [52] K. Wohlfeld, M. Daghofer, G. Khaliullin, and J. van den Brink, *J. Phys.: Conf. Ser.* **391**, 012168 (2012).
- [53] A. L. Chernyshev and M. E. Zhitomirsky, *Phys. Rev. B* **79**, 144416 (2009).
- [54] S. M. Winter, K. Riedl, P. A. Maksimov, A. L. Chernyshev, A. Honecker, and R. Valentí, *Nat. Commun.* **8**, 1152 (2017).
- [55] M. Takahashi, *Phys. Rev. B* **40**, 2494 (1989).
- [56] Z. Z. Du, H. M. Liu, Y. L. Xie, Q. H. Wang, and J.-M. Liu, *Phys. Rev. B* **92**, 214409 (2015).
- [57] A. S. Erickson, S. Misra, G. J. Miller, R. R. Gupta, Z. Schlesinger, W. A. Harrison, J. M. Kim, and I. R. Fisher, *Phys. Rev. Lett.* **99**, 016404 (2007).
- [58] M. Hosoi, T. Mizoguchi, T. Hinokihara, H. Matsuura, and M. Ogata, *arXiv:1804.04874*.